Flexible beta-Ga_2O_3 Nanomembrane Schottky Barrier Diodes

Edward Swinnich, Md Nazmul Hasan, Jung-Hun Seo*
Department of Materials Design and Innovation
University at Buffalo, SUNY
Buffalo, NY 14260
Email: edwardsw@buffalo.edu, mhasan9@buffalo.edu, *junghuns@buffalo.edu

***Abstract*— we have demonstrated high power flexible Schottky barrier diodes (SBDs) on a plastic substrate using single crystalline beta-Ga_2O_3 nanomembranes (NMs). In order to realize flexible high power beta-Ga_2O_3 SBDs, a sub-micron thick free-standing beta-Ga_2O_3 NMs were created from a bulk beta-Ga_2O_3 substrate and transfer-printed onto the plastic substrate via a micro-transfer printing method. It was revealed that the material property of beta-Ga_2O_3 NMs such as crystal structure, electron affinity, and bandgap remains unchanged compared with its bulk properties. Flexible beta-Ga_2O_3 SBDs exhibit the record high critical breakdown field strength (E_c) of 1.2 MV/cm in the flat condition and 1.07 MV/cm of E_c under the bending condition. Overall, flexible beta-Ga_2O_3 SBDs offer great promise for future flexible energy convergence systems and are expected to provide a much larger and more versatile platform to address a broader range of high-performance flexible applications.**

Keywords— beta-Ga_2O_3 nanomembrane; Flexible Schottky barrier diodes; High power flexible electronics

I. INTRODUCTION

Research in flexible electronics has been intensively conducted in the past decade and various flexible applications have been developed such as transistors, photodetectors, biosensors, photovoltaics, and energy harvesters. [1] In particular, highly flexible inorganic single crystalline semiconductors have been introduced, and these have electrical properties that are superior to those of other flexible semiconductors such as polymer, amorphous or polycrystalline semiconductors. [2] Therefore, the performance of inorganic semiconductor based flexible applications is approaching that of their rigid counterparts [3], which allows us to realize high-performance flexible electronics such as high-efficiency photovoltaics, microwave communication systems, implantable biomedical systems, and optoelectronic systems. [4] While some of these applications can form stand-alone flexible systems, many of these applications need multi-level configurations that require up- and down- convergence of power and signals. To simultaneously enable efficient power convergence functionality and good mechanical flexibility, specific requirements have to be fulfilled, such as a sufficiently large band gap (>3eV), high carrier mobility and critical breakdown electric field (μ>100 $cm^2/v{\cdot}s$ and Ec>1MV/cm), and most importantly, excellent flexibility and durability. Such flexible electronics will be referred to as high-power flexible electronics. High-power flexible electronics can provide superior performance and application advantages. As is known, high-power devices can handle a higher level of power (namely, voltage, current or both) with much thinner semiconductors, and this is a substantial benefit in the realization of flexible electronics, where the thickness of the material is closely related to their bendability. High-power flexible electronics also enable us to expand the capability of flexible electronics by offering a higher level of voltage or current, as well as efficient power convergence. However, the realization of flexible power electronics has been hindered by the absence of semiconductors that fulfill the aforementioned requirements.

In order to realize flexible high-power electronics, it is essential to use a thin form of wide bandgap semiconductors. In the past, free-standing SiC, GaN, and ZnO have been successfully developed into flexible electronics and optoelectronic applications. [5, 6] Recently, beta-phase Ga_2O_3 (β-Ga_2O_3) has attracted considerable attention as an emerging wide bandgap semiconductor beyond SiC and GaN due to its excellent material properties, such as an ultra-wide bandgap value (> 4.8eV), high carrier mobility (>300 $cm^2/v{\cdot}s$), and critical breakdown electric field (~8 MV/cm). [7] Furthermore, β-Ga_2O_3 exhibits the second highest critical electric field (Ec) and the highest electron-Baliga's Figure of Merit (B_{FoM}) of all wide bandgap semiconductors. More importantly, β-Ga_2O_3 can be processed to a sub-micron thin free-standing nanomembrane (NM), due to its highly anisotropic monoclinic crystal structure and unbalanced lattice constants [8]. While several rigid electronic applications based on β-Ga_2O_3 NMs have been demonstrated in past years [9], β-Ga_2O_3 based flexible electronics have not yet been demonstrated, due to the various technical challenges such as the high-temperature metallization process and difficulties in creating or relocating separated β-Ga_2O_3.In this paper, we report the first demonstration of flexible high-power switching devices on a plastic substrate using a printed single crystalline β-Ga_2O_3 NMs. In order to realize flexible high power β-Ga_2O_3 NM Schottky barrier diodes (SBDs), we have employed several technological innovations, that enable us to utilize the β-Ga_2O_3 NMs on a plastic substrate such as the employment of an inductively coupled plasma treatment process to achieve Ohmic contact to β-Ga_2O_3 NMs or the two step transfer-printing process to

enhance the quality, yield, and size of the created β-Ga_2O_3 NMs. Consequently, our flexible high power β-Ga_2O_3 NM SBDs exhibit the record high critical breakdown field strength (Ec) of 1.2 MV/cm in a flat condition and 1.07 MV/cm of Ec under a bending condition. The reported approach not only enables us to demonstrate various unique flexible applications, such as flexible energy-efficient power convergence devices and high-performance, flexible solar-blind photodetectors, but also gives us a higher degree of freedom in structure-property investigation by granting access to various crystal orientations using a transfer printing method.

II. Results and Discussion

Figure 1(a) presents a schematic illustration of the fabrication process of high power β-Ga_2O_3 NM SBDs on a flexible substrate. The details of the device fabrication process can be found in the method section, but in short, the fabrication starts from a mechanical cleaving of several large segments from bulk β-Ga_2O_3. Bulk β-Ga_2O_3 was grown by molecular beam epitaxy and lightly doped with Sn at 5×10^{17} cm^{-3} on the [201] direction. The β-Ga_2O_3 flakes, which have a relatively thick thickness in the range of 1~50 μm were exfoliated from the large β-Ga_2O_3 segment using a well-known micromechanical cleavage technique (also known as a "Scotch-tape" method) that is commonly used to create graphene from bulk graphite. As shown in Figure 1(a)(i), β-Ga_2O_3 was cleaved at an angle of 77° due to its highly anisotropic monoclinic crystal structure with a β angle of 103° [8], thus, following exfoliation, the crystal orientation of the cleaved surface is in the [100] direction. The exfoliated β-Ga_2O_3 flakes were further thinned on a SiO_2 substrate in order to create sub-micron thick β-Ga_2O_3 flakes (now it is called β-Ga_2O_3 NMs) by using a sonification process in isopropyl alcohol (Figure 1(a)(ii)-(iv)). Figure S1 in the supplementary information shows the statistical relationship between the thickness and width of the β-Ga_2O_3 NMs. Once the thinning process was completed, the β-Ga_2O_3 NMs were picked by an elastomeric stamp (Polydimethylsiloxane, PDMS; Silgard) and then carefully transfer-printed onto an adhesive coated plastic substrate (polyimide, PI; Sigma Aldrich), followed by a curing process to permanently bond the β-Ga_2O_3 NMs onto the plastic substrate (Figure 1(a)(v)). Figure 1(b) shows a microscopic image of a transfer-printed β-Ga_2O_3 NM on a PI substrate. The rainbow-colored bands on the surface of the β-Ga_2O_3 NM was attributed to particles trapped underneath of the β-Ga_2O_3 NM, but the surface of the β-Ga_2O_3 NMs itself are atomically smooth with root-mean-square roughness < ~1 nm as shown in Figure 1(c). After the completion of the bonding process, an Ohmic metal stack (Ti/Au) was deposited, and the plasma treatment was carried out prior to the deposition in order to achieve Ohmic contact without the need of an additional high-temperature annealing process (Figure 1(a)(vi)). Then, a Schottky metal stack (Ti/Pt/Au) was deposited to complete the fabrication of the device (Figure 1(a)(vii)). Figure 1(d) shows a microscopic image of the finished β-Ga_2O_3 SBDs. The sample was then ready for measurements of the electrical properties, as well as a bending test, in which tensile or compressive strain was applied to the device (Figure 1(a)(viii)).

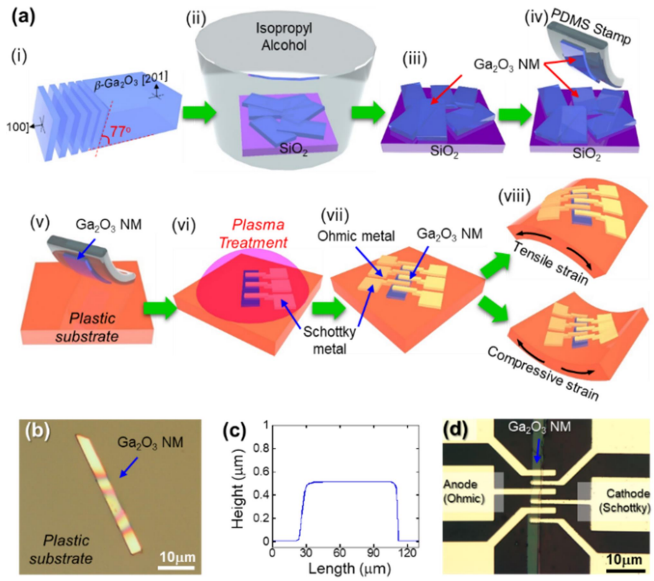

Figure 1. (a) an schematic illustration of the fabrication process for the β-Ga_2O_3 NMs SBD; (i) a cleaving process from the bulk β-Ga_2O_3, (ii)-(iii) additional sonification process to further thin down β-Ga_2O_3, (iv)-(v) a micro-transfer printing process to relocate the β-Ga_2O_3 NMs onto a plastic substrate, (vi)-(vii) metallization process for Ohmic and Schottky contacts. (viii) an illustration of the bending test. (b) a microscopic image of the transfer-printed β-Ga_2O_3 NMs on a plastic substrate which is responded to a step(v) in Figure 1(a). (c) a thickness profile of a typical β-Ga_2O_3 NMs on a plastic substrate, (d) a microscopic image of the finished β-Ga_2O_3 NM SBDs

Prior to fabricating the device, we investigated the quality of the β-Ga_2O_3 NMs, since they were not chemically synthesized, but mechanically exfoliated from a bulk substrate. It is well-known that strain can change the electrical and optical properties of semiconductors, and thus it was important to inspect the strain condition of the printed β-Ga_2O_3 NMs. Raman spectroscopy has been widely used to examine the strain condition of various materials and we compared the Raman spectrum from a bulk β-Ga_2O_3 to that of a printed β-Ga_2O_3 NM. Figure 2(a) shows the Raman spectra taken from the bulk β-Ga_2O_3 and the printed β-Ga_2O_3 NM. It is noted that the Raman intensity from the bulk β-Ga_2O_3 was much stronger than that of the printed β-Ga_2O_3 NM due to the difference in their physical thickness, and the spectra from the samples were normalized. The Raman modes of β-Ga_2O_3 can be classified into three major modes: (i) the low-frequency mode: a liberation and translation of Ga-O tetrahedra-octahedra chains (below 300 cm^{-1}), (ii) the mid-frequency mode: a deformation of GaO_2 octahedra (300 ~ 500 cm^{-1}), (iii) the high-frequency mode: a stretching and bending of GaO_4 tetrahedra, respectively. [10] As shown in the upper panel of Figure 2(a), ten Raman peaks were observed in our present study of bulk β-Ga_2O_3, and this is in good agreement with previous studies. [11] However, for the printed β-Ga_2O_3 NM, Raman peaks at 144 cm^{-1} and 320 cm^{-1} were not observed. The absence of these two characteristic peaks is attributed to different lattice vibration modes in the [201] and [100] crystal orientations. Also, no peaking shifting and the same full-width half

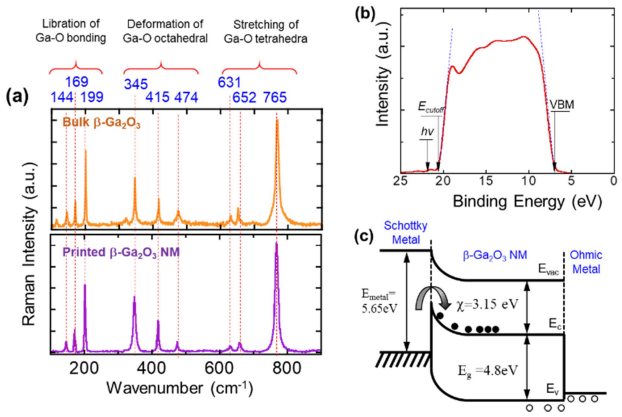

Figure 2. (a) Raman spectra taken from the bulk β-Ga_2O_3 and the printed β-Ga_2O_3 NMs showing no residual strain is remained, **(b)** a measured UPS spectrum taken from the printed β-Ga_2O_3 NMs to identify its' electron affinity value. **(c)** a re-constructed band diagram of the β-Ga_2O_3 NMs SBDs using measured/known

maximum of the Raman peaks between the bulk β-Ga_2O_3 and the β-Ga_2O_3 NM confirm that β-Ga_2O_3 NM does not experience any built-in strain during an exfoliation step and thus maintains high crystal quality.

Next, we carefully inspected the electronic structure of the printed β-Ga_2O_3 NM using an ultraviolet photoelectron spectroscopy (UPS) to determine its electron affinity. The UPS measurement was performed in an ultrahigh vacuum system equipped with a SPECS Microwave ultraviolet light source (He I = 21.2 eV; the UV light spot is about 1 mm in diameter). The UPS spectrum of the printed β-Ga_2O_3 NMs is shown in Figure 2(b). The electron affinity of the printed β-Ga_2O_3 NMs was calculated to be 3.15 eV using the following equation [12]:

$$\chi = (E_o - E_F) + (E_F - E_V) - E_G = (h\nu - E_{cutoff}) + (E_F - E_V) - E_G \quad (1)$$

where χ is the electron affinity of β-Ga_2O_3 NM, EF, EV, EG are the fermi-level, valence band, and band gap, respectively; and E_{cutoff} is the cutoff energy. The electron affinity of 3.15 eV for the printed β-Ga_2O_3 NMs is slightly smaller than that of the bulk β-Ga_2O_3 (which is typically about 4 eV ± 0.05 eV). Since their surface chemistries are different, we speculate that the smaller electron affinity of the printed β-Ga_2O_3 NMs might be due to the difference in the crystal orientation, which is [201] for the bulk β-Ga_2O_3 and [100] for the printed β-Ga_2O_3 NM. However, the difference in the electron affinity values of the bulk β-Ga_2O_3 and that of the β-Ga_2O_3 NM remain unknown and require further study for clarification. With the measured electron affinity of 3.15 eV and the known metal work function value, the Schottky barrier height was calculated to be 2.3 eV using the Schottky-Mott model, also known as the work-function model [13]:

$$\Phi_B = E_G - (\Phi_M - \chi) \quad (2)$$

where Φ_B is the Schottky barrier height, EG is the band gap, χ is the electron affinity of the β-Ga_2O_3 NM, and Φ_M is the metal work function (5.65 eV for the Pt). Both the electron affinity and Schottky barrier height calculations used a E_G of 4.8eV for β-Ga_2O_3 NM; this was determined by UV-vis spectrophotometry in an earlier study. [14] Finally, the band diagram of the flexible β-Ga_2O_3 NM SBDs was constructed, as illustrated in Figure 2(c) and the measured barrier height is large enough for the current rectification in β-Ga_2O_3 NM SBDs.

The electrical characterization of β-Ga_2O_3 NM SBDs was carried out using a Keithley 4200 semiconductor parameter analyzer. Figure 3 shows the I-V characteristics of the β-Ga_2O_3 NM SBDs under different bending conditions using convex and concave molds that have different curve radii from 110 mm to 20 mm which corresponds to up to 0.33% of the tensile strain (for the convex mold) and up to 0.19% of the compressive uniaxial strain (for the concave mold). The bending test was first performed on the concave mold to apply uniaxial compressive strains from the flat condition to 0.06%, 0.09%, and 0.19%, followed by uniaxial tensile strains from the flat condition to 0.09%, 0.13%, 0.19%, and 0.33%, respectively. In the flat condition prior to the initial bending, the devices exhibited good rectifying behavior with an on/off ratio of over 10^6 which is similar to the rigid version of the β-Ga_2O_3 SBDs as measured by others. [9]. The ideality factor and series resistance were calculated to be 1.28 and 140 Ω, respectively using thermionic emission theory. [13]. However, the I-V characteristics were degraded under both compressive and tensile uniaxial strains. As shown in Figure 3(a), both forward and reverse current were decreased under compressive uniaxial strain, and in particular, the reverse current was decreased by a factor of 250, and the degraded I-V characteristics did not recover to the initial values of the flat condition. A similar trend was observed with the β-Ga_2O_3 NM SBDs under the tensile uniaxial strain condition as shown in Figure 3(b). Interestingly, once the I-V characteristics had been degraded by the initial bending, the I-V curves experienced no further degradation following additional bending. Figure 3(c) summarizes the changes in forward and reverse current taken at

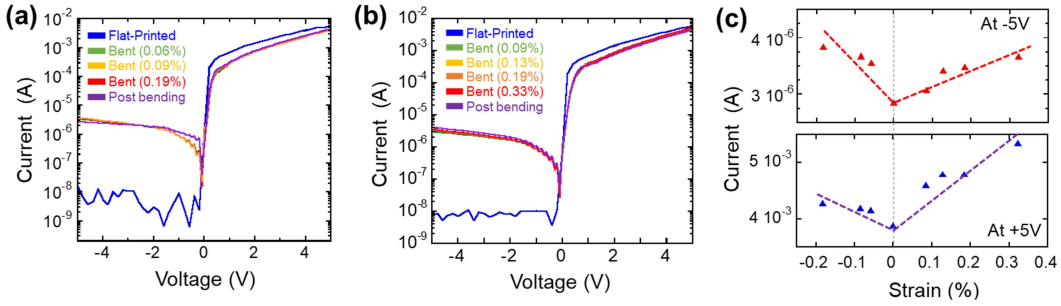

Figure 3. I-V characteristics flexible β-Ga_2O_3 NMs SBDs on a plastic substrate under **(a)** compressive strains, and **(b)** tensile strains. **(c)** a reverse and a forward current measured at -5V (top) and +5V (bottom) as a function of bending induced external strain.

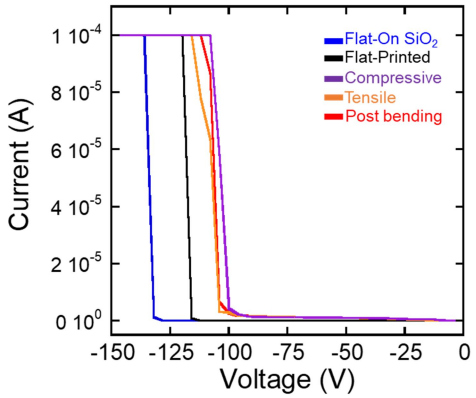

Figure 4. The breakdown voltage (V_{BR}) of the flexible β-Ga_2O_3 SBDs in a flat condition and under bending condition. The inset shows a logarithm scale of I-V characteristics.

-5V and +5V as a function of strain. The current level was increased up to 20% when measured under the strain condition at ±5V; this is attributed to the changes in the effective mass and scattering rate due to the external strain. As a result, carrier mobility is enhanced under the strain condition.

Finally, we investigated the breakdown voltage (V_{BR}) of the flexible β-Ga_2O_3 SBDs when flat and under bending. The V_{BR} measurement was carried out using a Keithley 2651 high power source meter at room temperature. The current compliance was set to 100 μA to protect the devices from a sudden electric breakdown at high reverse bias voltages. Figure 4 shows the V_{BR} characterization under bending using the same convex and concave molds that were used for the low voltage I-V characterization. The V_{BR} of the flexible β-Ga_2O_3 SBDs in the flat condition (prior to the initial bending) reached about -119V which corresponds to the critical breakdown field strength (Ec) of 1.2 MV/cm and a $R_{ON,SP}$ of 0.58 mΩ·cm^2, resulting in a Baliga's figure of merit (FOM) of 98 MW/cm^2. The V_{BR}, however, decreased to -102V (Ec=1.03 MV/cm) and -104V (Ec=1.04 MV/cm) under 0.2% of compressive strain and 0.33% of tensile strain, respectively. The degradation in V_{BR} remained the same as for -101V in the flat condition after the initial bending. To compare the V_{BR} of flexible β-Ga_2O_3 SBDs with the rigid version of β-Ga_2O_3 SBD, we fabricated β-Ga_2O_3 SBDs on SiO_2 substrate using the same Ohmic and Schottky metal stacks. The reference rigid version of β-Ga_2O_3 SBDs exhibited much higher V_{BR} (-136V) than that of the flexible version of β-Ga_2O_3 SBDs (-119V). The difference in V_{BR} between the rigid version and the flexible version of β-Ga_2O_3 SBDs is attributed to different thermal conductivity (k) of the substrates ($k_{polyimide}$=0.12 W/m·K versus k_{SiO2}=1.5 W/m·K).

III. Conclusions

In conclusion, flexible β-Ga_2O_3 based SBDs were successfully fabricated and the electrical characterization was observed under bending conditions. We observed a sudden decrease in current under bending conditions, for both compressive and tensile strains. Although this performance degradation does not recover when the material returns to the flat condition, a mild thermal annealing process can improve the performance. Finally, the breakdown voltage was measured for both flat and bending conditions, and the flexible β-Ga_2O_3 SBDs exhibited a breakdown voltage of -119 V, which corresponds to the critical breakdown field strength of 1.2 MV/cm. Overall, flexible β-Ga_2O_3 based SBDs offer great promises for high-performance and future flexible energy convergence systems, and they are expected to provide a versatile flexible platform with complex functions that can address a broad range of unique applications particularly in airborne/space surveillance applications.

Acknowledgment

This work was supported by the National Science Foundation (ECCS- 1809077) and partially by the seed grant by Research and Education in energy, Environment and Water (RENEW) Institute at the University at Buffalo.

References

[1] K. Nomura, H. Ohta, A. Takagi, T. Kamiya, M. Hirano, H. Hosono, "Room-temperature fabrication of transparent flexible thin-film transistors using amorphous oxide semiconductors", Nature Vol. 432, pp. 488, 2004.

[2] J. A. Rogers, M. G. Lagally, R. G. Nuzzo, "Synthesis, assembly and applications of semiconductor nanomembranes", Nature Vol. 477, pp. 45, 2011.

[3] J.-H. Seo, T. Ling, S. Gong, W. Zhou, A. L. Ma, L. J. Guo, Z. Ma, "Fast flexible transistors with a nanotrench structure", Sci. Rep., Vol. 6, pp. 24771, 2016.

[4] J. Yoon, S. Jo, I. S. Chun, I. Jung, H.-S. Kim, M. Meitl, E. Menard, X. Li, J. J. Coleman, U. Paik, J. A. Rogers, "GaAs photovoltaics and optoelectronics using releasable multilayer epitaxial assemblies", Nature, Vol. 465, pp. 329, 2010.

[5] R. Könenkamp, R. C. Word, M. Godinez, "Ultraviolet electroluminescence from ZnO/polymer heterojunction light-emitting diodes", Nano Lett., Vol. 5, pp. 2005, 2005.

[6] K. Xiong, S. H. Park, J. Song, G. Yuan, D. Chen, B. Leung, J. Han, "Single crystal gallium nitride nanomembrane photoconductor and field effect transistor", Adv. Funct. Mater., Vol. 24, pp. 6503, 2014.

[7] S. J. Pearton, J. Yang, P. H. Cary, F. Ren, J. Kim, M. J. Tadjer, M. A. Mastro, "A review of Ga2O3 materials, processing, and devices", Applied Physics Reviews, Vol. 5, pp. 011301, 2018.

[8] W. S. Hwang, A. Verma, H. Peelaers, V. Protasenko, S. Rouvimov, H. Xing, A. Seabaugh, W. Haensch, C. V. de Walle, Z. Galazka, M. Albrecht, R. Fornari, D. Jena, "High-voltage field effect transistors with wide-bandgap β-Ga2O3 nanomembranes", Appl. Phys. Lett., Vol. 104, pp. 203111, 2014.

[9] H. Zhou, K. Maize, G. Qiu, A. Shakouri, P. D. Ye, "β-Ga2O3 on insulator field-effect transistors with drain currents exceeding 1.5 A/mm and their self-heating effect", Appl. Phys. Lett., Vol. 111, pp. 092102, 2017.

[10] D. Dohy, G. Lucazeau, A. Revcolevschi, "Raman spectra and valence force field of single-crystalline β Ga2O3", Journal of Solid State Chemistry, Vol. 45, pp. 180, 1982.

[11] J. Li, X. Chen, Z. Qiao, M. He, H. Li, "Large-scale synthesis of single-crystalline β-Ga2O3 nanoribbons, nanosheets and nanowires", J. Phys. Condens. Matter, Vol. 13, pp. L937, 2001.

[12] W. M. Haynes, CRC handbook of chemistry and physics, CRC press, 2014.

[13] S. M. Sze, K. K. Ng, Physics of semiconductor devices, John wiley & sons, 2006.

[14] E. Swinnich, Y. J. Dave, E. B. Pitman, S. Broderick, B. Mazumder, J.-H. Seo, "Prediction of optical band gap of β-(AlxGa1-x) 2O3 using material informatics", Materials Discovery, Vol. 11, pp. 1, 2018